Polyhedron 29 (2010) 2643–2650

Contents lists available at ScienceDirect

Polyhedron

journal homepage: www.elsevier.com/locate/poly

Syntheses, EPR spectral studies and crystal structures of manganese(II) complexes of neutral *N,N* donor bidentate Schiff bases and azide/thiocyanate as coligand

Sreesha Sasi [a], M. Sithambaresan [a], M.R. Prathapachandra Kurup [a,*], H.-K. Fun [b]

[a] Department of Applied Chemistry, Cochin University of Science and Technology, Kochi 682 022, Kerala, India
[b] X-ray Crystallography Unit, School of Physics, Universiti Sains Malaysia, Peneng, Malaysia

ARTICLE INFO

Article history:
Received 3 November 2009
Accepted 10 June 2010
Available online 20 June 2010

Keywords:
Crystal structure
Schiff bases
Mn(II) complex
Azide
Thiocyanate
EPR spectra

ABSTRACT

Four manganese(II) complexes $Mn_2(paa)_2(N_3)_4$ (**1**), $[Mn(paa)_2(NCS)_2]\cdot{}^3/_2H_2O$ (**2**), $Mn(papea)_2(NCS)_2$ (**3**), $[Mn(dpka)_2(NCS)_2]\cdot{}^1/_2H_2O$ (**4**) of three neutral *N,N* donor bidentate Schiff bases were synthesized and physico-chemically characterized by means of partial elemental analyses, electronic, infrared and EPR spectral studies. Compounds **3** and **4** were obtained as single crystals suitable for X-ray diffraction. Compound **4** recrystallized as $Mn(dpka)_2(NCS)_2$. Both the compounds crystallized in the monoclinic space groups $P2_1$ for **3** and $C2/c$ for **4**. Manganese(II) is found to be in a distorted octahedral geometry in both the monomeric complexes with thiocyanate anion as a terminal ligand coordinating through the nitrogen atom. EPR spectra in DMF solutions at 77 K show hyperfine sextets with low intensity forbidden lines lying between each of the two main hyperfine lines and the zero field splitting parameters (D and E) were calculated.

1. Introduction

Manganese complexes play important roles ranging from bioinorganic chemistry to solid-state physics. There has been considerable interest in synthesizing biomimetic complexes that can act as manganese containing enzymes such as superoxide dismutase (SOD) [1]. Interest in manganese complexes of varying nuclearities continues to be stimulated by the presence of manganese at the active sites of biological systems such as photosystem II in green plants, ribonucleotide reductase, superoxide dismutase, and the Mn catalases [2–9], the variability in magnetic behavior of polynuclear manganese clusters, which for some systems has been exploited in the development of information storage devices [10–12] and the use of such complexes as catalysts for bleaching and organic synthesis [13–15].

In manganese biosystems, the azide ion is known to inhibit the superoxide dismutation in mononuclear superoxide dismutases *via* binding to the metal at the active site in both the Mn(II) and Mn(III) oxidation states [16]. The function of dinuclear active sites in Mn catalases, which catalyze the conversion of toxic peroxide to oxygen and water in certain bacteria, is also dramatically inhibited by azide [17–22].

Gao et al. reports the structure and magnetism of Mn(II) one dimensional coordination polymers built from azide bridges and Schiff base obtained by the condensation of pyridine-2-carbaldehyde with aniline and its derivatives [23]. The complexes synthesized contain alternating end-on and end-to-end azide bridges, which mediate alternating ferromagnetic and antiferromagnetic exchange interactions, respectively. Wen and coworkers prepared one dimensional chiral coordination polymers of manganese(II) using azide and a Schiff base (obtained from pyridine-2-carbaldehyde and 1-phenylethyl amine) as the auxiliary ligand [24]. In these complexes, there is weak antiferromagnetic coupling between Mn(II) ions. The use of di-2-pyridyl ketone in conjugation with dicyanamide and azide gave cubane and defective double-cubane clusters of Mn(II) respectively, both of which are found to be antiferromagnetic in nature [25,26]. The use of Schiff base ligands in conjugation with groups *viz.* azide, thiocyanate etc. can give interesting results. In this context, we report the syntheses, structural and spectral characteristics of four Mn(II) complexes of the Schiff bases obtained by the condensation of pyridine-2-carbaldehyde with aniline, *R*-1-phenylethyl amine with aniline and di-2-pyridyl ketone with aniline. Azide and thiocyanate anions are used as coligands in these complexes.

2. Experimental

2.1. Materials

Pyridine-2-carbaldehyde (Sigma–Aldrich), di-2-pyridyl ketone (Sigma–Aldrich), aniline (S.D. Fine), *R*-1-phenylethyl amine (Alfa

* Corresponding author. Tel.: +91 484 2575804; fax: +91 484 2577595.
E-mail address: mrp@cusat.ac.in (M.R.P. Kurup).

0277-5387/$ - see front matter © 2010 Elsevier Ltd. All rights reserved.
doi:10.1016/j.poly.2010.06.006

Aeser), $Mn(ClO_4)_2{\cdot}6H_2O$ (Sigma–Aldrich), $Mn(OAc)_2{\cdot}4H_2O$ (Merck), $MnCl_2{\cdot}4H_2O$ (Sigma–Aldrich), NaN_3 (Reidel-De Haen), KCNS (BDH) and methanol (Merck) were used as received.

Caution! Although not encountered in our experiments, azide complexes are potentially explosive. Only a small amount of the material should be prepared, and it should be handled with care.

2.2. Syntheses of ligands

The Schiff bases (Scheme 1) were prepared *in situ* according to the literature methods for analogous compounds [27].

2.3. Syntheses of complexes

2.3.1. Synthesis of $Mn_2(paa)_2(N_3)_4$ (**1**)

A mixture of pyridine-2-carbaldehyde (0.107 g, 1 mmol) and aniline (0.093 g, 1 mmol) in methanol was refluxed for 2 h. To this, $Mn(ClO_4)_2{\cdot}6H_2O$ (0.362 g, 1 mmol) dissolved in methanol was added and stirred followed by the slow addition of an aqueous solution of NaN_3 (0.130 g, 2 mmol). The resulting solution was further stirred for 15 min to obtain an orange precipitate. It was then filtered, washed with water, methanol and finally with ether and dried over P_4O_{10} *in vacuo*. Elemental *Anal.* Calc. (%): C, 44.54; H, 3.14; N, 34.70. Found: C, 44.87; H, 3.14; N, 34.89%. μ = 5.06 BM. Main IR bands: 2095vs, 2058vs, 1589m, 1442m, 1329m, 1013m, 689w, 638w, 481w.

2.3.2. Synthesis of $[Mn(paa)_2(NCS)_2]{\cdot}^3/_2H_2O$ (**2**)

A mixture of pyridine-2-carbaldehyde (0.107 g, 1 mmol) and aniline (0.093 g, 1 mmol) in methanol was refluxed for 2 h. $Mn(OAc)_2{\cdot}4H_2O$ (0.245 g, 1 mmol) dissolved in methanol and solid KCNS (0.194 g, 2 mmol) was added to this and refluxed for 4 h. A pale brown solid separated out after two days from the reaction mixture, which was filtered, washed with water, methanol and ether and dried over P_4O_{10} *in vacuo*. Elemental *Anal.* Calc. (%): C, 54.93; H, 3.69; N, 15.42; S, 12.25, Found: C, 55.51; H, 4.12; N, 14.94; S, 11.40%. μ = 6.05 BM. Main IR bands: 3446b, 2062vs, 1593m, 1486m, 1013m, 775w, 694m, 543m, 411w.

2.3.3. Synthesis of $Mn(papea)_2(NCS)_2$ (**3**)

Pyridine-2-carbaldehyde (0.107 g, 1 mmol) and *R*-1-phenylethyl amine (0.121 g, 1 mmol) was refluxed in methanol for 2 h. A methanolic solution of $MnCl_2{\cdot}4H_2O$ (0.198 g, 1 mmol) and solid KCNS (0.194 g, 2 mmol) was added to this and refluxed for 4 h. The yellow single crystals suitable for X-ray diffraction were isolated within two days in appreciable yield, which were mechanically separated and dried. Elemental *Anal.* Calc. (%): C, 60.64 (60.90); H, 4.66 (4.77); N, 14.16 (14.20). Found: C, 60.90; H, 4.77; N, 14.20%. μ = 5.92 BM. Main IR bands: 2069vs, 2053vs, 1594m, 1440m, 1384m, 1013m, 789w, 764w, 637m, 497w, 413w.

2.3.4. Synthesis of $[Mn(dpka)_2(NCS)_2]{\cdot}^1/_2H_2O$ (**4**)

Di-2-pyridyl ketone (0.187 g, 1 mmol) was dissolved in methanol and aniline (0.093 g, 1 mmol) was added to this. About 4–5 drops of glacial acetic acid was also added and refluxed for 6 h. To the above solution, $Mn(OAc)_2{\cdot}4H_2O$ (0.245 g, 1 mmol) dissolved in methanol was added. An aqueous solution of KCNS (0.194 g, 2 mmol) was also added. The resulting solution was refluxed for 2 h. An orange colored crystalline product was obtained within a week, filtered, washed with ether and dried over P_4O_{10} *in vacuo*. The filtrate on evaporation yielded orange X-ray quality single crystals of $Mn(dpka)_2(NCS)_2$. Elemental *Anal.* Calc. (%): C, 61.77 (61.88); H, 3.82 (3.89); N, 16.10 (16.04). Found: C, 61.88; H, 3.89; N, 16.04%. μ = 5.73 BM. Main IR bands: 2063vs, 2041vs, 1579m, 1475m, 1015m, 623m, 409w.

2.4. Physical measurements

Elemental analyses of the complexes were done on a Vario EL III CHNS analyzer at SAIF, Kochi, India. The IR spectra were recorded on a Thermo Nicolet AVATAR 370 DTGS model FT-IR spectrophotometer with KBr pellets at SAIF, Kochi. Electronic spectra of the complexes in acetonitrile solution were recorded on a Spectro UV–VIS Double Beam UVD-3500 spectrometer in the 200–900 nm range. The EPR spectra of the complexes were recorded on a Varian E-112 spectrometer using TCNE as the standard, with 100 kHz modulation frequencies and 0.2 mT modulation amplitude at the SAIF, IIT, Bombay, India. The magnetic susceptibility measurements were carried out at the Indian Institute of Technology, Roorkee, India, at room temperature in the polycrystalline state on a PAR model 155 Vibrating Sample Magnetometer at 5 kOe field strength.

2.5. X-ray crystallography

Single crystal X-ray diffraction measurements of complexes **3** and **4** were carried out on a Bruker Smart Apex 2 CCD area detector diffractometer at the X-ray Crystallography Unit, School of Physics, Universiti Sains Malaysia, Penang, Malaysia. The unit cell parameters were determined and the data collections were performed using a graphite-monochromated Mo Kα (λ = 0.71073 Å) radiation at a detector distance of 5 cm at 100(1) K with the Oxford Cyrosystem Cobra low-temperature attachment. The collected data were reduced using SAINT program [28] and the empirical absorption corrections were performed using SADABS program [28]. The structures were solved by direct methods and refinement was carried out by full-matrix least squares on F^2 using the SHELXTL software package [29]. All non-hydrogen atoms were refined anisotropically. Hydrogen atoms were geometrically fixed at calculated positions and allowed to ride on their parent

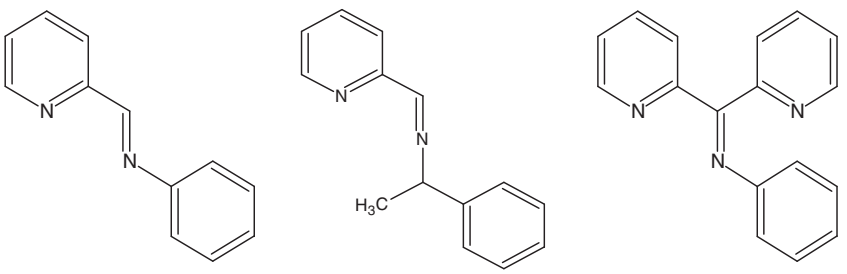

paa papea dpka

Scheme 1. Structures of Schiff bases.

atoms. Molecular graphics employed were ORTEP-III [30] and DIAMOND [31]. Pertinent crystallographic data and structure refinement parameters are summarized in Table 1.

3. Results and discussion

The condensation of aldehyde/ketone and amine in 1:1 M ratio yielded the Schiff base ligands, which were used without further purification for the synthesis of the complexes by reaction with the metal salts in presence of pseudohalides NaN_3/KCNS. We were successful in obtaining the single crystals of complexes **3** and **4**. Even after repeated trails, all our attempts to isolate good quality single crystals of the other complexes went in vain. All the complexes had the Schiff bases as neutral bidentate *N,N* donor ligands. A compound with the same empirical formula as that of compound **1** has been synthesized previously [23]. But the work emphasized the magnetic studies and the magnetostructural correlations of the compound with out any EPR spectral studies. In this paper we are reporting the EPR spectral investigations of the complex. Even though the Schiff base obtained by the condensation between di-2-pyridyl ketone and aniline has an additional N atom, that N is not coordinated to the metal as evidenced by the crystal studies of **4**.

Table 1
Crystallographic data and structure refinement parameters.

Parameters	**3**	**4**
Empirical formula	$C_{30}H_{28}MnN_6S_2$	$C_{36}H_{26}MnN_8S_2$
Formula weight (*M*)	591.64	689.71
Crystal colour, crystal morphology	Yellow, block	Orange, slab
Temperature (*T*) (K)	100.0(1)	100.0(1)
Wavelength (Mo Kα) (Å)	0.71073	0.71073
Crystal system	Monoclinic	Monoclinic
Space group	$P2_1$ (No. 4)	$C2/c$ (No. 15)
Unit cell dimensions		
a (Å)	9.0040(2)	13.4724(2)
b (Å)	15.1618(3)	11.4583(2)
c (Å)	11.2770(2)	22.0778(4)
α (°)	90.00	90.00
β (°)	109.3800(10)	93.5380(10)
γ (°)	90.00	90.00
V (Å^3)	1452.27(5)	3401.67(10)
Z	2	4
D_{calc} (ρ) (mg m^{-3})	1.353	1.347
Absorption coefficient, μ (mm^{-1})	0.629	0.549
F(0 0 0)	614	1420
Crystal size (mm^3)	0.69 × 0.40 × 0.28	0.35 × 0.31 × 0.17
θ Range (°)	1.91–35.00	1.85–35.00
Limiting indices	$-14 \leqslant h \leqslant 13$ $-24 \leqslant k \leqslant 24$ $-18 \leqslant l \leqslant 18$	$-21 \leqslant h \leqslant 21$ $-18 \leqslant k \leqslant 18$ $-34 \leqslant l \leqslant 35$
Reflections collected/unique	48582/12743 [*R*(int) = 0.0213]	30578/7447 [*R*(int) = 0.0535]
Completeness to 2θ = 35.00	100%	99.4%
Absorption correction	SADABS	SADABS
Maximum and minimum transmission	0.8432 and 0.6724	0.9129 and 0.8306
Refinement method	Full-matrix least-squares on F^2	Full-matrix least-squares on F^2
Data/restraints/parameters	12743/1/352	7447/0/213
Goodness-of-fit (GOF) on F^2	1.022	1.051
Final *R* indices [$I > 2\sigma(I)$]	R_1 = 0.0287, wR_2 = 0.0764	R_1 = 0.0464, wR_2 = 0.1123
R indices (all data)	R_1 = 0.0301, wR_2 = 0.0774	R_1 = 0.0725, wR_2 = 0.1307
Largest difference in peak and hole(e Å^{-3})	1.141 and −0.992	0.595 and −0.388

$wR_2 = \{\Sigma[w(F_o^2 - F_c^2)^2]/\Sigma[w(F_o^2)^2]\}^{1/2}$.
$R_1 = \Sigma||F_o| - |F_c||/\Sigma|F_o|$.

The room temperature magnetic susceptibility measurements of the compounds **1–4** showed values for magnetic moments in the range 5.73–6.05 BM, which are indicative of a high spin d^5 system [32]. The magnetic moment of compound **1** had a lower value, probably because of exchange interaction between the metal centers. All the complexes were found to be soluble in DMF, DMSO and acetonitrile, but only partially soluble in other organic solvents such as $CHCl_3$, ethanol and methanol.

3.1. Crystal structure of $Mn(papea)_2(NCS)_2$ (**3**)

The molecular structure of the complex along with the atom-numbering scheme is given in Fig. 1. The complex crystallizes into a monoclinic crystal system with two molecules in the unit cell. Selected bond lengths and bond angles are listed in Table 2. The complex crystallizes in the chiral space group $P2_1$ (No. 4) and the molecule is chiral due to the asymmetric nature of the Schiff base ligand. The ligand retains its configuration in the complex as well. Based on R and S configuration due to Cahn-Ingold-Prelog, the carbon atoms C7 and C21 have the R configuration, as is the case with the starting amine (*R*-1-phenylethyl amine). Mn(II) is in a distorted octahedral environment, which is occupied by four nitrogen atoms (N1, N2, N3 and N4) from two chelating bidentate Schiff base ligands papea and two nitrogens (N5 and N6) from two thiocyanate ions. The coordination polyhedron consists of MnN_6 chromophore with pairs of *trans* pyridyl N (N1 and N3), *cis* azomethine N (N2 and N4) and *cis* thiocyanate N (N5 and N6) atoms. The thiocyanate ions are coordinated in terminal manner *via* the nitrogen atom.

The bond lengths and bond angles reveal significant distortion from the ideal octahedral geometry. The rather small bite angle [N3–Mn1–N4 = 72.13(3)°] defines the largest distortion of the geometry. The thiocyanates which are almost linear [N5–C29–S1 = 178.00(11)° and N6–C30–S2 = 178.77(11)°] are coordinated to Mn(II) in a bent fashion [Mn1–N5–C29 = 157.95(10)° and Mn1–N6–C30 = 139.21(8)°]. These structural features are in agreement with that observed in other structurally characterised complexes containing terminally N-bound thiocyanate groups [33–38]. The Mn(II)–N bond length is shortest for thiocyanate nitrogens, indicating their stronger coordination than the pyridyl and azomethine nitrogens of the Schiff base. Mn–$N_{pyridyl}$ and Mn–N_{NCS} bond lengths are similar to the ones reported for similar Mn(II)-thiocyanate monomeric complexes [35–38]. Mn–$N_{pyridyl}$ and Mn–$N_{azomethine}$ bond distances are also comparable to Mn(II)

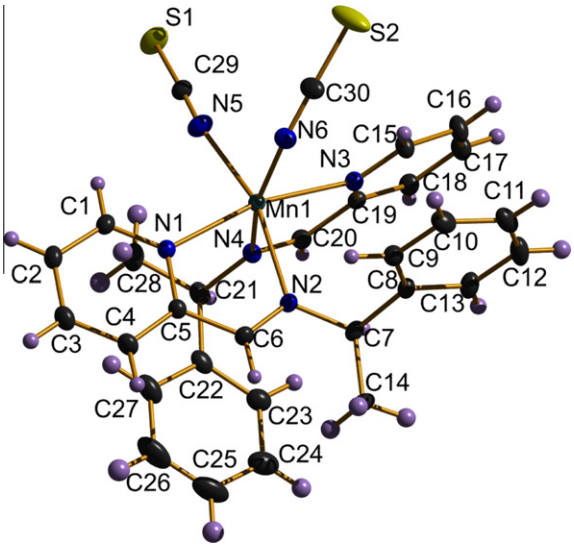

Fig. 1. The molecular structure of $Mn(papea)_2(NCS)_2$ **(3)** along with the atom-numbering scheme.

Table 2
Selected bond lengths (Å) and bond angles (°).

3		**4**	
Bond lengths (Å)			
Mn1–N1	2.2871(8)	Mn1–N1	2.3084(11)
Mn1–N2	2.2819(9)	Mn1–N1#1	2.3084(11)
Mn1–N3	2.2927(8)	Mn1–N3	2.2785(11)
Mn1–N4	2.3775(8)	Mn1–N3#1	2.2785(11)
Mn1–N5	2.1389(11)	Mn1–N4	2.1194(13)
Mn1–N6	2.1639(9)	Mn1–N4#1	2.1194(13)
N5–C29	1.1640(15)	N4–C18	1.1687(19)
N6–C30	1.1676(14)	S1–C18	1.6230(15)
S1–C29	1.6291(11)		
S2–C30	1.6294(12)		
N1–C5	1.3502(13)		
N2–C6	1.2763(13)		
C5–C6	1.4717(14)		
N3–C19	1.3523(11)		
N4–C20	1.2768(11)		
C19–C20	1.4690(12)		
Bond angles (°)			
N1–Mn1–N2	72.71(3)	N4#1–Mn1–N4	100.32(7)
N1–Mn1–N3	166.42(3)	N4#1–Mn1–N3	101.08(5)
N1–Mn1–N4	100.08(3)	N4–Mn1–N3	97.85(5)
N1–Mn1–N5	92.91(4)	N4#1–Mn1–N3#1	97.85(5)
N1–Mn1–N6	98.22(3)	N4–Mn1–N3#1	101.08(5)
N2–Mn1–N3	95.46(3)	N3–Mn1–N3#1	150.27(6)
N2–Mn1–N4	87.32(3)	N4#1–Mn1–N1	86.44(5)
N2–Mn1–N5	162.33(4)	N4#1–Mn1–N1	168.13(5)
N2–Mn1–N6	101.01(3)	N3–Mn1–N1	71.12(4)
N3–Mn1–N4	72.13(3)	N3#1–Mn1–N1	87.51(4)
N3–Mn1–N5	97.38(4)	N4#1–Mn1–N1#1	168.13(5)
N3–Mn1–N6	90.47(3)	N4–Mn1– N1#1	86.44(5)
N4–Mn1–N5	85.13(4)	N3–Mn1– N1#1	87.51(4)
N4–Mn1–N6	161.46(3)	N3#1–Mn1–N1#1	71.12(4)
N5–Mn1–N6	91.00(4)	N1#1–Mn1–N1#1	88.65(6)
Mn1–N5–C29	157.95(11)	C18–N4–Mn1	164.68(12)
Mn1–N6–C30	139.20(9)	N4–C18–S1	178.50(14)
S1–C29–N5	178.01(11)		
S2–C30–N6	178.77(11)		

Symmetry transformations used to generate equivalent atoms: #1 = $-x, y, -z + 1/2$.

complexes of some thiosemicarbazones reported previously [39–42]. However these distances are slightly longer than those for the polymeric Mn(II)-azido complex using the same Schiff base [24]. Also the bond distances of the Schiff base in the complex are similar to those previously reported [24]. The mean plane deviation calculations show that the metal-chelate rings are almost planar. Ring puckering analysis [43] reveals that the metal chelate ring Cg(2) comprising of Mn1, N3, C19, C20 and N4 can be best described as being twisted on Mn1–N3 bond [$Q(2) = 0.1000(8)$ Å and $\Phi = 189.4162(5876)°$].

The packing in the crystal lattice (Fig. 2) is in an ABAB.... manner, which when repeated, one dimensionally forms a layer and the successive layers arranged in a similar manner. No classical hydrogen bonds are observed in the crystal structure. The packing of the molecules in the crystal lattice is stabilized by C–H···π interactions and the weak π···π interactions (Table 3). A weak C7–H7A(1)···Cg(2) ring interaction comprised of Mn1, N3, C19, C20 and N4 atoms [with a H···Cg distance of 2.92 Å and an angle of 114°] stabilizes each molecule, while the π···π interactions between the rings Cg(1) comprised of Mn1, N1, C5, C6 and N2 atoms and Cg(6) comprised of C22, C23, C24, C25, C26 and C27 atoms [with a distance of 3.9557(7) Å between the ring centroids] reinforces the crystal structure cohesion in the packing.

3.2. Crystal structure of $Mn(dpka)_2(NCS)_2$ (**4**)

The molecular structure of the complex along with the atom-numbering scheme is given in Fig. 3. The complex crystallizes in a monoclinic crystal system with four molecules in the unit cell. Selected bond lengths and bond angles are listed in Table 2.

The molecule is centrosymmetric and the structure consists of a neutral monomer in which the manganese(II) ions are octahedrally coordinated by two dpka ligands (through N1 and N3) and two terminal NCS^- ligands (through N4). The pyridyl N atoms of the two Schiff bases, N3 are *trans*-located, while the azomethine N atoms (N1) and the thiocyanate N atoms N4 are *cis*-located in the complex. The N atoms (N2) present on the second pyridyl ring are not coordinated to Mn(II). The Mn–N distance is shortest for the thiocyanate nitrogens and longest for the azomethine nitrogens. The MnN_6 octahedra exhibit a noticeable distortion from the regular geometry. The rather small bite angle of 71.12(4)° corresponding to the N3–Mn–N1 bond angle signifies the extent of distortion. The thiocyanate groups are coordinated in terminal manner to the Mn(II) atom through the nitrogen atom. The NCS groups are quasi-linear with an N4–C18–S1 bond angle of 178.50(14)° and are bonded to the Mn(II) ion through an angle of 164.68(12)°. The Mn–N bond distances are in agreement with the previous reports [25,26,33–38,44]. Mean plane deviation calculations show that the metal-chelate rings are almost planar.

The Mn–N bond distances in compound **4** are smaller than that in **3** for the pyridyl and thiocyanate nitrogens. For the azomethine nitrogens, the Mn–N bond distance is longer in one of the Schiff bases in compound **3**, but shorter in the other Schiff base coordinated to the manganese when compared with those in **4**. The average $Mn–N_{NCS}$ bond distances are almost identical in the two complexes.

The packing of the molecules of **4** in the crystal lattice (Fig. 4) is in a head to tail manner. Classical hydrogen bonds are absent. The molecules are connected in the crystal lattice through a weak hydrogen bond interaction C(16)–H(16A)···N(2) [with a H···N distance of 2.5888 Å and an angle of 139.34°] leading to a three dimensional network. The network of electron delocalization brought about by the aromatic and metallo-aromatic [45] rings gives rise to diverse π···π and C–H···π interactions, invoking stable molecular arrangement in the unit cell. The interaction parameters are listed in Table 3. The assembly of molecules is in such a manner that there are cavities in the crystal lattice which are formed as a result of π···π and C–H···π interactions.

3.3. Infrared and electronic spectra

The IR spectra of the four complexes are quite similar. The ν(C=N) absorption characteristic of the azomethine group of the Schiff base ligands occurs at *ca.* 1585 cm^{-1} as a medium band for all the complexes. The position of this band is in agreement with the previous reports and is thus indicative of the coordination of azomethine N [23,46]. The medium band at *ca.* 1450 cm^{-1} is attributed to pyridyl ring stretching and the medium band at *ca.* 1013 cm^{-1} is due to pyridyl ring breathing. The in-plane ring deformation of the pyridyl ring and the pyridyl ring out-of-plane bending are observed at frequencies 600–700 and 400–500 cm^{-1}, respectively. The above observations indicate the pyridyl N coordination. The IR data are in conformity with the previous reports dealing with complexes having similar ligand systems [24].

The most interesting part of the spectra of all the complexes is the region above 2000 cm^{-1}, where the absorptions due to pseudohalogens are observed. In compound **1**, in the 2000–2100 cm^{-1} region expected for the $\nu_{as}(N_3)$ absorption, the occurrence of two sharp and strong bands at 2058 and 2095 cm^{-1} indicates the presence of two different coordinated azido groups. Such higher wavenumbers of the $\nu_{as}(N_3)$ stretching is probably due to the presence of bridging azides. But in the absence of crystal structure, it is impossible to draw definite conclusions. The medium band at *ca.* 1329 cm^{-1} is assignable to the azido

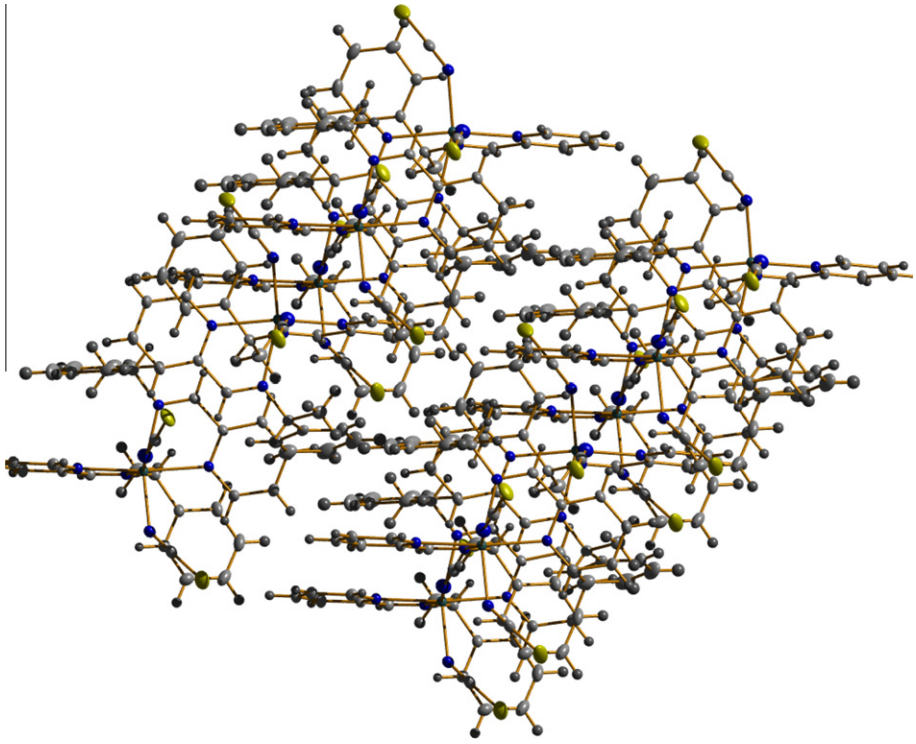

Fig. 2. Packing diagram of compound (**3**) viewed down the '*b*' axis.

Table 3
H-bonding, C–H···π and π···π interaction parameters.

D–H···A	D–H (Å)	H···A (Å)	D···A (Å)	D-H···A (°)
H-bonding				
3				
C(16)–H(16A)··· N(2)[a]	0.9298	2.5888	3.349(2)	139.34
Equivalent position code: a = 1/2-x,-1/2 + y, 1/2-z				
C–H(I)···Cg(J)	H···Cg (Å)	C–H···Cg (°)	C···Cg (Å)	
C–H···π interactions				
3				
C7–H7A(1)···Cg(2)	2.92	114 Cg(2) = Mn1, N3, C19, C20, N4	3.4382(12)	
4				
C2–H2A(1)···Cg(1)[b]	3.1811	99.37	3.4562(16)	
C2–H2A(1)···Cg(2)[c]	3.1811	99.37	3.4562(16)	
C3–H3A(1)···Cg(4)[d]	2.9932	139.68	3.7511(18)	
C8–H8A(1)···Cg(5)[e]	3.1013	165.06	4.008(2)	
Equivalent position codes: b = −x, y, 1/2−z; c = x, y, z d = −1/2 + x, 1/2 + y, z; e = −x, 1−y, 1−z		Cg(1) = Mn1, N1, C12, C13, N3 Cg(2) = Mn1, N1#, C12#, C13#, N3# Cg(4) = N3, C13, C14, C15, C16, C17 Cg(5) = C1, C2, C3, C4, C5, C6		
Cg(I)···Cg(J)	Cg···Cg (Å)	α°	β°	γ°
π···π interactions				
3				
Cg(1)···Cg(6)	3.9557(7)	8.53	23.26	29.56
Cg(6)···Cg(1)	3.9557(7)	8.53	29.56	23.26
		Cg(1) = Mn1, N1, C5, C6, N2 Cg(6) = C22, C23, C24, C25, C26, C27		
4				
Cg(1)···Cg(1)[f]	3.1650(7)	88.93	59.19	59.19
Cg(1)···Cg(2)[g]	3.1650(7)	88.93	59.19	59.19
Cg(2)···Cg(1)[g]	3.1650(7)	88.93	59.19	59.19
Cg(2)···Cg(2)[f]	3.1650(7)	88.93	59.19	59.19
Cg(4)···Cg(5)[f]	3.8637(9)	20.08	27.35	25.47
Cg(5)···Cg(4)[f]	3.8635(9)	20.08	25.47	27.35
Equivalent position codes: *f* = –*x*, *y*, 1/2 − *z*, *g* = *x*, *y*, *z*		Cg(1) = Mn1, N1, C12, C13, N3 Cg(2) = Mn1, N1#, C12#, C13#, N3# Cg(4) = N3, C13, C14, C15, C16, C17 Cg(5) = C1, C2, C3, C4, C5, C6		

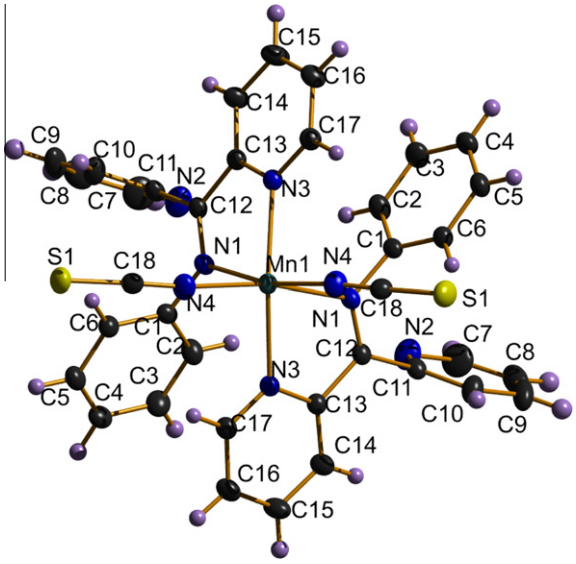

Fig. 3. The molecular structure of $Mn(dpka)_2(NCS)_2$ **(4)** along with the atom-numbering scheme.

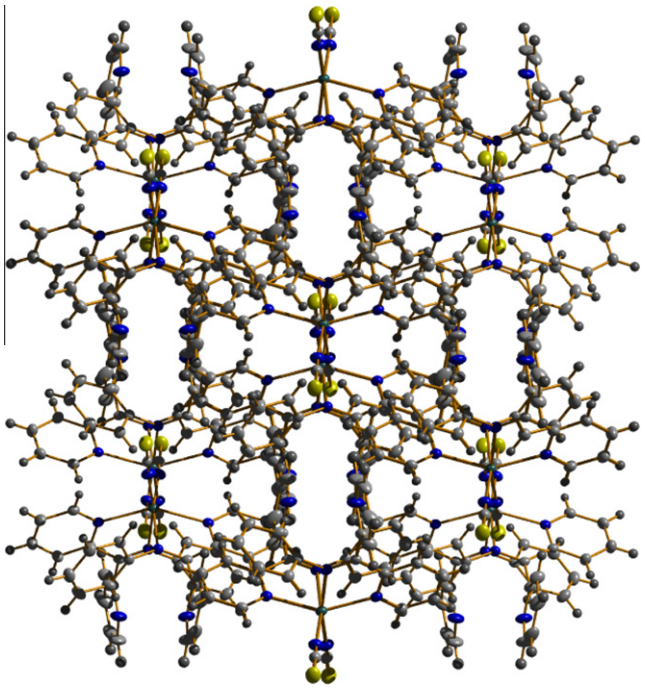

Fig. 4. Packing diagram of compound (**4**) viewed down the 'c' axis.

symmetric stretching mode, $\nu_s(N_3)$ [47]. The deformation mode of the azido ligand is observed as a weak band at 689 cm^{-1}.

The presence of a single strong band at 2062 cm^{-1} in the region of ν_{as}(C=N) absorption in compound **2** indicates the existence equivalent N-bonded thiocyanates. This points out to the possibility of *trans* location of the thiocyanate groups. The ν(CS) is found at 775 cm^{-1} and the δ(NCS) bending mode is obtained at 543 cm^{-1} confirming the existence of N-bonded NCS group. In the IR spectrum of compounds **3** and **4**, there are two strong and sharp peaks at *ca.* 2065 and 2045 cm^{-1}, which are assignable to the ν_{as}(C=N) stretching of the thiocyanate groups. This indicates the existence of two non-equivalent coordinated thiocyanate groups and hence mutual *cis* coordination. The thiocyanate groups are terminal and are coordinated to the metal *via* N.

The ground state of high-spin octahedrally coordinated Mn(II) complex is $^6A_{1g}$. The absence of any other spin sextet terms requires that all transitions in high spin d^5 complexes are spin forbidden. Also for octahedral complexes, transitions are Laporte forbidden. Thus doubly forbidden transitions are extremely weak. In the complexes **1–4**, the *d–d* bands could not be identified due to their extremely low intensity. The $\pi \rightarrow \pi^*$ transitions are observed as intense peaks at *ca.* 290 nm and the $n \rightarrow \pi^*$ transitions of the ligand are seen as intense peaks *ca.* 310–335 nm. The charge transfer bands are observed at 400 nm. The electronic spectral assignments are summarized in Table 4.

3.4. EPR spectra

The spin Hamiltonian for Mn(II) may be described by the spin Hamiltonian

$$\hat{H} = g\beta BS + D[S_z^2 - S(S+1)/3] + E(S_x^2 - S_y^2)$$

where B is the magnetic field vector, D is the axial zero field splitting term, E is the rhombic zero field splitting parameter, g is the g-factor, β the Bohr Magneton and S is the electron spin vector [48]. If D and E are very small compared to $g\beta BS$, five EPR transitions corresponding to $\Delta m_s = \pm 1$, *viz.*, $|+5/2> \leftrightarrow |+3/2>$, $|+3/2> \leftrightarrow |+1/2>$, $|+1/2> \leftrightarrow |-1/2>$, $|-1/2> \leftrightarrow |-3/2>$ and $|-3/2> \leftrightarrow |-5/2>$ are expected with a g value of 2.0. However, for the case where D or E is very large, the lowest doublet has effective g values of $g_{||} = 2$, $g_{\perp} = 6$ for $D \neq 0$ and $E = 0$ but for $D = 0$ and $E \neq 0$, the middle Kramers doublet has an isotropic g value of 4.29 [49,50].

The EPR spectral parameters of all the complexes are listed in Table 5. The solid state EPR spectrum of complex **1** at 298 K is characterized by a broad signal with g value of 2.009. However, in the spectrum of **2**, in addition to the signal at 2.018, there is another broad weak signal with g value of ~4.324. The solid state EPR spectra of **3** and **4** at 77 K displayed three signals including low field signals at 5.794 and 4.569, respectively. The three g values indicate that the Mn(II) in these complexes are rhombically distorted. The signals of **3** and **4** were very broad due to dipolar interactions and a random orientation of the Mn^{2+} ions [49]. Manganese hyperfine splitting is not observed in the solid state spectra of any of these complexes. In the spectra from DMF solutions at 77 K, a hyperfine sextet is observed for **1**, **2**, **3** and **4**. The six hyperfine lines are due to the interaction of the electron spin with the nuclear spin (^{55}Mn, $I = 5/2$). For complexes **1** and **2**, a broad signal in the low field region is also observed with g values of ~4.353 and ~5.778, respectively. All the spectra taken in DMF at 77 K of these complexes were simulated using EasySpin [51] and they are represented in Figs. 5–8.

The observed g values are very close to the free electron spin value, suggestive of the absence of spin orbit coupling in the ground state. Also they are in agreement with the values reported previously for structurally similar Mn(II) complexes and is indicative of the distorted octahedral geometry of Mn(II) [38]. The A values are consistent with an octahedral coordination, since A in tetrahedral sites is 20–25% lower than in octahedral sites. The A values are

Table 4
Electronic spectral data for Mn(II) complexes.

Compound	$\pi \rightarrow \pi^*$ (nm)	$n \rightarrow \pi^*$ (nm)	CT (nm)
$Mn_2(paa)_2(N_3)_4$ (**1**)	291	310	400
$[Mn(paa)_2(NCS)_2]\cdot{}^3/_2H_2O$ (**2**)	292	310	390
$Mn(papea)_2(NCS)_2$ (**3**)	294	315	400
$Mn(dpka)_2(NCS)_2\cdot{}^1/_2H_2O$ (**4**)	289	325	410

Table 5
EPR spectral parameters for Mn(II) complexes.

Compound	Polycrystalline state		Solution (DMF) g_{iso} (77 K)	A_{iso}(MHz)	D (MHz)	E (MHz)	E/D
	g (298 K)	g (77 K)					
1	2.009		1.991	256.4	400	110	0.275
2	2.018		1.992	248.1	420	170	0.404
3		$g_1 = 1.939$ $g_2 = 2.821$	2.001	330.5	490	110	0.224
4		$g_1 = 1.960$ $g_2 = 2.681$	2.035	299.1	380	80	0.210

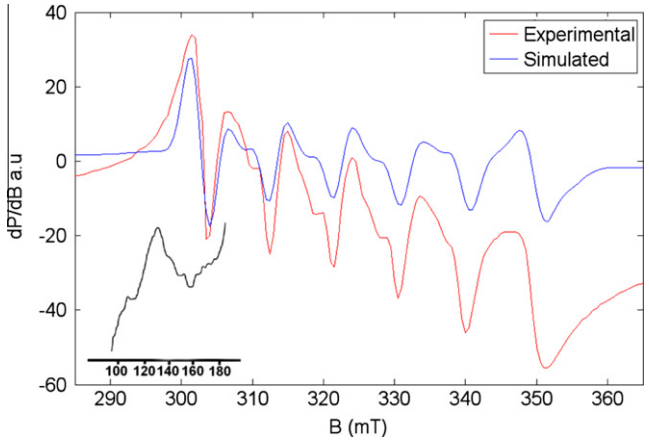

Fig. 5. EPR spectrum of $Mn_2(paa)_2(N_3)_4$ (**1**) in DMF at 77 K. Spectrum in the lower field region is given in the inset.

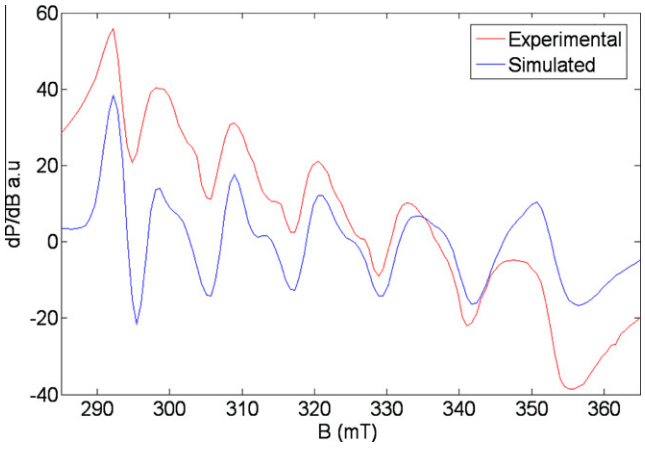

Fig. 7. EPR spectrum of $Mn(papea)_2(NCS)_2$ (**3**) in DMF at 77 K.

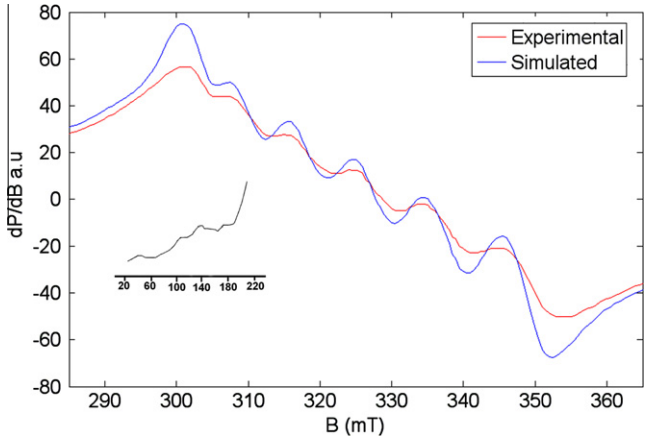

Fig. 6. EPR spectrum of $[Mn(paa)_2(NCS)_2]\cdot{}^3/_2H_2O$ (**2**) in DMF at 77 K. Spectrum in the lower field region is given in the inset.

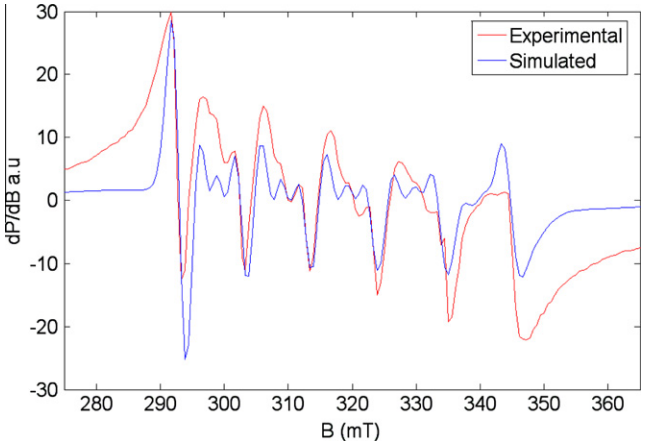

Fig. 8. EPR spectrum of $Mn(dpka)_2(NCS)_2\cdot{}^1/_2H_2O$ (**4**) in DMF at 77 K.

somewhat lower than pure ionic compounds, which reflects the covalent nature of the metal–ligand bonds in the complexes. The mixing of the nuclear hyperfine levels with the zero field splitting factor of the Hamiltonian (D and E) produces low intensity forbidden lines lying between each of the two main hyperfine lines in the frozen solution spectra of the complexes **1**, **3** and **4** [52]. Axial splitting factor D and the rhombic splitting factor E were calculated for the complexes **1**, **2**, **3** and **4**. The forbidden peaks are not visible in complex **2** due to broadening of the main hyperfine lines in the spectrum. The E/D ratio is significantly affected by the geometry and the coordination number of the complex. It varies from pure axial systems ($E/D = 0$) to close rhombic ones ($E/D = 1/3$) and it mostly depends on the nature of the neutral ligands [53]. E/D ratios of these complexes are consistent with the reported values of distorted octahedral and five-coordinated Mn(II) complexes [53,54]. However, no conclusion can be drawn from the grater deviation of the ratio of the complex **2** from that of the other complexes.

4. Supplementary data

CCDC 287861 and 744574 contain the supplementary crystallographic data for $Mn(papea)_2(NCS)_2$ and $Mn(dpka)_2(NCS)_2$. These data can be obtained free of charge via http://www.ccdc.cam.ac.uk/conts/retrieving.html, or from the Cambridge Crystallographic

Data Centre, 12 Union Road, Cambridge CB2 1EZ, UK; fax: (+44) 1223-336-033; or e-mail: deposit@ccdc.cam.ac.uk.

Acknowledgement

Sreesha Sasi thanks the CSIR, New Delhi, India for financial support in the form of a fellowship. M. Sithambaresan thanks the ICCR for financial support. H.-K. Fun thanks Universiti Sains Malaysia for the Fundamental Research Grant Scheme [FRGS] grant No. 203/PFIZIK/671064. The authors are thankful to the Sophisticated Analytical Instruments Facility, Kochi, India for the elemental analyses.

References

[1] J.M. McCord, I. Fridovich, J. Biol. Chem. 244 (1969) 6049.
[2] K. Wieghardt, Angew. Chem., Int. Ed. Engl. 28 (1989) 1153.
[3] V.K. Yachandra, K. Sauer, M.P. Klein, Chem. Rev. 96 (1996) 2927.
[4] W. Rüttinger, G.C. Dismukes, Chem. Rev. 97 (1997) 1.
[5] C. Tommos, G.T. Babcock, Acc. Chem. Res. 31 (1998) 18.
[6] V.L. Pecoraro, M.J. Baldwin, A. Gelasco, Chem. Rev. 94 (1994) 807.
[7] G.C. Dismukes, Chem. Rev. 96 (1996) 2929.
[8] M.L. Ludwig, A.L. Metzger, K.A. Pattridge, W.C. Stallings, J. Biol. Chem. 219 (1991) 335.
[9] D.P. Riley, P.J. Lennon, W.L. Neumann, R.H. Weiss, J. Am. Chem. Soc. 119 (1997) 6522.
[10] R. Sessoli, H.-L. Tsai, A.R. Schake, S. Wang, J.B. Vincent, K. Folding, D. Gatteschi, G. Christou, D.N. Hendrickson, J. Am. Chem. Soc. 115 (1993) 1804.
[11] E.M. Chudnovsky, Science 274 (1996) 938.
[12] S.M.J. Aubin, Z. Sun, I.A. Guzei, A.L. Rheingold, G. Christou, D.N. Hendrickson, Chem. Commun. (1997) 2239.
[13] R. Hage, J.E. Iburg, J. Kerschner, J.H. Koek, E.L.M. Lempers, R.J. Martens, U.S. Racherla, S.W. Russell, T. Swarthoff, M.R.P. van Vliet, J.B. Warnaar, L. van der Wolf, B. Krljen, Science 369 (1994) 637.
[14] D.E. de Vos, T.J. Ben, Organomet. Chem. 195 (1996) 520.
[15] C. Zondervan, R. Hage, B.L. Ferigna, Chem. Commun. (1997) 419.
[16] J.W. Whittaker, M.M. Whittaker, J. Am. Chem. Soc. 113 (1991) 5528.
[17] Y. Kono, I. Fridovich, J. Bacteriol. 155 (1983) 742.
[18] Y. Kono, I. Fridovich, J. Biol. Chem. 258 (1983) 6015.
[19] W.F. Beyer Jr., I. Fridovich, Biochemistry 24 (1985) 6460.
[20] R.M. Fronko, J.E. Penner-Hahn, C.J. Bender, J. Am. Chem. Soc. 110 (1988) 7554.
[21] G.S. Waldo, R.M. Fronko, J.E. Penner-Hahn, Biochemistry 30 (1991) 10486.
[22] G.S. Waldo, S. Yu, J.E. Penner-Hahn, J. Am. Chem. Soc. 114 (1992) 5869.
[23] E.-Q. Gao, S.-Q. Bai, Y.-F. Yue, Z.-M. Wang, C.-H. Yan, Inorg. Chem. 39 (2003) 3642.
[24] H.-R. Wen, C.-F. Wang, Y. Song, J.-L. Zuo, X.-Z. You, Inorg. Chem. 44 (2005) 9039.
[25] G.S. Papaefstathiou, A. Escuer, F.A. Mautner, C. Raptopoulou, A. Terzis, S.P. Perlepes, R. Vicente, Eur. J. Inorg. Chem. (2005) 879.
[26] G.S. Papaefstathiou, A. Escuer, C.P. Raptopoulou, A. Terzis, S.P. Perlepes, R. Vicente, Eur. J. Inorg. Chem. (2001) 1567.
[27] P. Bamfield, R. Price, R.G.J. Miller, J. Chem. Soc. A (1969) 1447.
[28] Bruker APEX2 Version 1.27, SAINT Version 7.12a and SADABS Version 2004/1, Bruker AXS, Madison, WI, USA, 2005.
[29] G.M. Sheldrick, SHELXTL Version 5.10, Bruker AXS Inc., Madison, Wisconsin, USA, 1998.
[30] L.J. Farrugia, J. Appl. Cryst. 30 (1997) 565.
[31] K. Bradenburg, H. Putz, DIAMOND Version 3.0, Crystal Impact, GbR, Postfach 1251, D-53002 Bonn, Germany, 2004.
[32] F.A. Cotton, G. Wilkinson, C.A. Murillo, M. Bochmann, Advanced Inorganic Chemistry, sixth ed., Wiley, New York, 1999. p. 839.
[33] M.A.S. Goher, F.A. Mautner, Polyhedron 12 (1993) 1863.
[34] M.-G. Zhao, J.-M. Shi, C.-J. Wu, Z. Kristallogr. 218 (2003) 157.
[35] G. De Munno, G. Viau, M. Julve, F. Lloret, J. Faus, Inorg. Chim. Acta 257 (1997) 121.
[36] M.G. Barandika, M.L. Hernández-Pino, M.K. Urtiaga, R. Cortés, L. Lezama, M.I. Arriortua, T. Rojo, J. Chem. Soc., Dalton Trans. (2000) 1469.
[37] S.K. Chattopadhyay, K. Mitra, S. Biswas, C.R. Lucas, D.O. Miller, B. Adhikary, J. Coord. Chem. 55 (2002) 1409.
[38] K. Mitra, S. Biswas, S.K. Chattopadhyay, B. Adhikary, C.R. Lucas, Transition Met. Chem. 30 (2005) 185.
[39] A. Sreekanth, M. Joseph, H.-K. Fun, M.R.P. Kurup, Polyhedron 25 (2006) 1408.
[40] A. Usman, I.A. Razak, S. Chantrapromma, H.-K. Fun, A. Sreekanth, S. Sivakumar, M.R.P. Kurup, Acta Crystallogr., Sect. C 58 (2002) m461.
[41] V. Philip, V. Suni, M.R.P. Kurup, M. Nethaji, Spectrochim. Acta Part A 64 (2006) 171.
[42] P.F. Rapheal, E. Manoj, M.R.P. Kurup, Polyhedron 26 (2007) 5088.
[43] D. Cremer, J.A. Pople, J. Am. Chem. Soc. 97 (1975) 1354.
[44] P. Bhunia, B. Baruri, U. Ray, C. Sinha, S. Das, J. Cheng, T.-H. Lu, Transition Met. Chem. 31 (2006) 310.
[45] H. Masui, Coord. Chem. Rev. 219 (2001) 957.
[46] E.-Q. Gao, Y.-F. Yue, S.-Q. Bai, Z. He, C.-H. Yan, Cryst. Growth Des. 5 (2005) 1119.
[47] S.S. Tandon, L.K. Thompson, M.E. Manuel, J.N. Bridson, Inorg. Chem. 22 (1994) 5555.
[48] D.J.E. Ingram, Spectroscopy at Radio and Microwave Frequencies, second ed., Butterworth, London, 1967.
[49] B.S. Garg, M.R.P. Kurup, S.K. Jain, Y.K. Bhoon, Transition Met. Chem. 13 (1988) 92.
[50] K.B. Pandeya, R. Singh, P.K. Mathur, R.P. Singh, Transition Met. Chem. 11 (1986) 347.
[51] S. Stoll, A. Schweiger, J. Magn. Reson. 178 (2006) 42.
[52] W. Linert, F. Renz, R. Boca, J. Coord. Chem. 40 (1996) 293.
[53] C. Mantel, C. Baffert, I. Romero, A. Deronzier, J. Pecaut, M. Collomb, C. Duboc, Inorg. Chem. C 43 (2004) 6455.
[54] C. Duboc, T. Phoeung, S. Zein, J. Pécaut, M.-N. Collomb, F. Neese, Inorg. Chem. 46 (2007) 4905.